TRENDS IN SCIENCES 2026; 23(3): 11548
https://doi.org/10.48048/tis.2026.11548 RESEARCH ARTICLE

Synthesis and Characterization of Nano AlN Powder from $Al(OH)_3$/C Precursors Using a Hybrid Method Carbothermal Reduction Nitridation—Hydrothermal Autoclave Assisted

I Kadek Ervan Hadi Wiryanta[1,4], Wayan Nata Septiadi[2,*], Tjokorda Gde Tirta Nindhia[2] and I Made Joni[3]

[1]*Study Program of Doctor Engineering Science, Faculty of Engineering, Udayana University, Bali 80361, Indonesia*
[2]*Study Program of Mechanical Engineering, Engineering Faculty, Udayana University, Bali 80361, Indonesia*
[3]*Department of Physics, Faculty of Mathematics and Natural Sciences, Universitas Padjadjaran, Sumedang 45363, Indonesia*
[4]*Mechanical Engineering Department, Politeknik Negeri Bali, Jalan Kampus Bukit Jimbaran, Bali 80364, Indonesia*

([*]Corresponding author's e-mail: wayan.nata@unud.ac.id)

Received: 9 August 2025, Revised: 12 September 2025, Accepted: 5 October 2025, Published: 10 December 2025

Abstract

A novel synthesized method using a hydrothermal autoclave assists in the carbothermal reduction nitridation (CRN) was developed to synthesize aluminum nitride (AlN) from $Al(OH)_3$ and carbon black as a starting material. The mass ratio of $Al(OH)_3$:C varies from 3:1, 4:1 and 5:1. N_2 gas with the flow rate of 0.1 L/min is flowed into an autoclave in the nitridation process with temperatures of 250, 300 and 350 °C. The characterization of synthesized AlN was observed using FTIR, XRD, SEM, PSA and UV-Vis. The FTIR results indicate that with a mass ratio of 3:1, the absorption peak was about ~488 cm^{-1}, which was the highest compared to mass ratio 4:1 (~485 cm^{-1}) and mass ratio 5:1 (~480 cm^{-1}). The success rate of synthesis is influenced by the increase in nitridation temperature. At a nitridation temperature of 350 °C, XRD results showed the formation of a homogeneous and crystalline AlN phase with an average crystallite size of about ~10.5 nm and a total crystallization percentage of 67.04%. Further SEM and PSA results verified the growth of nanostructures and reduced aggregation particles with an average size about ~125 nm. In addition, the UV-Vis spectroscopy revealed an optical bandgap of approximately 5.6 eV, aligning well with the typical semiconductor behavior of AlN.

Keywords: Aluminium nitride (AlN), $Al(OH)_3$, Carbon black, Hydrothermal autoclave, CRN

Introduction

Aluminium nitride (AlN) is a semiconductor associated with Group III-V, characterized by a wurtzite structure. AlN was first synthesized in 1877 and remained in production until the mid-1980s. AlN demonstrates a melting point of 2,800 °C at 100 atm and decomposes in a vacuum at 1,800 °C [1]. AlN is currently in great demand in the industry attributed to its inherent thermal conductivity (~285 W/m.K), broad energy bandgap (6.0 - 6.2 eV), robust chemical resistance and thermal expansion coefficient, which make it appropriate for applications in thermal management, UV optoelectronics, and as reinforcement in phase-change materials (PCM). The integration of AlN into PCM can boost heat conductivity and form stability, reduce leakage and improve mechanical strength, addressing the primary disadvantage of organic PCM. [2-4]. The main issue related to the aluminium nitride nanomaterial is its restricted availability and comparatively high cost, leading to efforts in synthesize AlN more efficiently.

In recent years, various methods for synthesizing aluminum nitride have been carried out, i.e., gas

nitridation [5], thermal plasma [6], sol-gel [7], electric explosion wire (EEW) [8], direct nitridation [9] and carbothermal reduction nitridation (CRN) [10]. The use of a plasma reactor in synthesizing AlN has an advantage in the morphology structure and the size of AlN, but it needs a high-energy reactor (~12 - 25 kW), which can be a drawback of the process. In direct nitridation methods, the resulting AlN powder has a high purity but also has a tendency to produce large particles due to the incomplete nitridation [11].

CRN methods are becoming dominant methods for AlN synthesis through its improved phase purity and regulated particle size distribution [12]. In the CRN process, several factors affect the synthesis results, including the preparation method of the raw material [13,14] and the use of additive substances [15,16]. Nevertheless, CRN generally requires excessive reactions temperatures (> 1,200 - 1,500 °C), which increases energy consumption, decreases efficiency and encourages particle agglomeration, therefore limiting its application.

The most popular source of aluminum raw materials in the AlN synthesis process currently is used aluminum hydroxide ($Al(OH)_3$), which has a higher nitriding reaction rate than Al_2O_3.

The basic reaction of CRN, which utilizes aluminum oxide (Al_2O_3) and carbon (C) as preccursor, could be described as:

$$Al_2O_3(s)+3C(s)+N_2(g) \rightarrow 2AlN(s)+3CO(g) \quad (1)$$

The synthesis of aluminium nitride (AlN) from aluminium hydroxide requires several reaction stages, specifically the decomposition of aluminium hydroxide ($Al(OH)_3$) into aluminium oxide (Al_2O_3), followed by reduction and nitridation. The reaction could be expressed as:

$$2Al(OH)_3(s)+3C(s)+N_2(g) \rightarrow 2AlN(s)+3CO(g)+3H_2O(g) \quad (2)$$

AlN synthesis utilizing aluminium hydroxide and carbon as precursors is influenced by several factors, including reaction temperature, gas flow rate, grain size, and the molar ratio of C/$Al(OH)_3$. Increasing the reaction temperature and molar ratio will enhance the reaction rate [17]. The extensive use of the CRN approach led to enhancement efforts, including nitridation techniques to yield improved AlN, as well as modifications in techniques to lower synthesis temperature [18-19].

The hydrothermal method is one of the best methods for creating a variety of nanomaterials and nanocomposites since it is inexpensive, easy to use and environmentally benign and it requires a modest synthesis temperature. A comprehensive study of the synthesis and analysis of oxide nanoparticles and their derivatives via hydrothermal growth is provided. This study demonstrates that nanoparticles of superior crystal quality can be synthesized by hydrothermal methods as a cost-effective approach [20]. The form and structure of the resulting nanomaterials can be adjusted by controlling the hydrothermal process duration [21].

Hydrothermal synthesis provides a unique advantage by reducing $Al(OH)_3$ into a very porous γ-Al_2O_3 or boehmite (AlOOH) precursor, highlighted by many surface –OH groups and defect sites, which exhibit significantly greater reactivity compared to stable α-Al_2O_3. This technique, when integrated with a carbon source under hydrothermal conditions, enables uniform mixing, hence minimizing diffusion distance and decreasing activation energy during nitridation [22-24]. Hydrothermal synthesis has been effectively utilized in other oxide systems, including TiO_2 and ZnO, to produce nanosized particles with adjustable shape and improved reactivity [25,26]. Another result of the hybrid technique combining carbothermal reduction and hydrothermal synthesis of hollow AlN microspheres indicates that the hydrothermal precursor can lower the temperature of nitridation compared to conventional CRN [27]. These investigations highlight the adaptability of hydrothermal treatment in modifying precursor characteristics, especially morphology and defective surfaces, which are essential for further nitridation or catalytic processes. Considering these advancements, most reported hydrothermal-assisted methods for AlN synthesis still necessitate rather high nitridation temperatures (> 1,200 - 1,400 °C) to attain full conversion. Extensive research focused on crystalline nanoscale AlN at ultra-low temperatures (≤ 400 °C) is still limited.

Although AlN has been thoroughly investigated, there is limited study integrating hydrothermal reaction with carbothermal reduction–nitridation for the lower-temperature synthesis of crystalline AlN. Prior

methodologies depend exclusively on CRN at higher temperatures or on solution-based techniques that produce amorphous intermediates requiring further calcination procedures. Consequently, the development of a hybrid technique that lowers the synthesis temperature while yielding crystalline, uniformly distributed AlN nanoparticles is of considerable significance.

Therefore, in this study, aluminum nitride synthesis was carried out using a hybrid method between carbothermal reduction nitridation (CRN) combined with the hydrothermal technique using an autoclave. The CRN method is utilized due to its ability to synthesize aluminum nitride in small and homogeneous particle sizes as well as its simpler procedure. In an attempt to be more energy efficient, the nitriding process, which needs high temperatures, can be completed at a lower temperature range with the aid of hydrothermal procedures that use an autoclave. In CRN methods, carbon black and aluminum hydroxide ($Al(OH)_3$) were employed as precursors, while the nitridation process used N_2 gas. The effect of precursor mass ratio ($Al(OH)_3$:C = 3:1, 4:1, 5:1) and processing temperature (250 - 350 °C) on the phase composition is further discussed.

Materials and methods

Experimental procedure

Commercial $Al(OH)_3$ and carbon black were used as precursors. $Al(OH)_3$ with the particle size < 150 μm (100 mesh) was used as the Al source. Carbon black with a particle size of 100 mesh was used as the C source and N_2 gas was used in the nitridation process as the N source. The mass ratio of the precursor varies with the ratios of $Al(OH)_3$:C at 3:1, 4:1 and 5:1. The synthesis results were characterized using FTIR to identify the optimal mass ratio variation. The nitridation temperature in hydrothermal autoclaves is varied at 250, 300 and 350 °C, based on the optimal mass ratio (FTIR screening result), to determine the most effective nitridation temperature for AlN synthesis utilizing a CRN-hydrothermal autoclave-assisted method. This range was selected intentionally as a preliminary report/proof-of-concept investigation to verify the potential of hydrothermal autoclave-assisted CRN in lowering the synthesis temperature of AlN. **Table 1** shows the details of sample composition.

Table 1 Precursors composition.

No	Mass ratio $Al(OH_3)$: C	$Al(OH)_3$ (g)	C (g)	Ethanol (mL)	Nitridation temperature (°C)	N_2 gas (L/min)
1	5 : 1	5	1	80	300	0.1
2	4 : 1	4	1	80	300	0.1
3	3 : 1	3	1	80	300	0.1
4	3 : 1	3	1	80	350	0.1
5	3 : 1	3	1	80	250	0.1

Synthesis of nano-aluminum nitride

The aluminum nitride synthesis process begins by mixing $Al(OH)_3$ and carbon black in a predetermined ratio and dissolving them using ethanol. Magnetic stirrer used to mix the precursor at room temperature and 850 rpm for 15 min to form slurries. In order to get dry slurries, the slurries are then put into an oven dryer for 3 h (180 min) at a temperature of 100 °C. The dried slurries then start the nitridation process using a hydrothermal autoclave. The nitridation process involves heating the slurries in the hydrothermal autoclave at a predetermined temperature. Nitrogen gas is introduced into the autoclave at a flow rate of 0.1 L/min as the nitrogen source. The nitridation process using the hydrothermal autoclave lasts for 60 min and produces gray-colored AlN powder. Next, a calcination process was carried out to remove residual carbon from the AlN. The calcination process was performed in a muffle furnace at a temperature of 700 °C for 5 h. The entire AlN synthesis process using a CRN method—hydrothermal autoclave assisted—is illustrated in **Figure 1**.

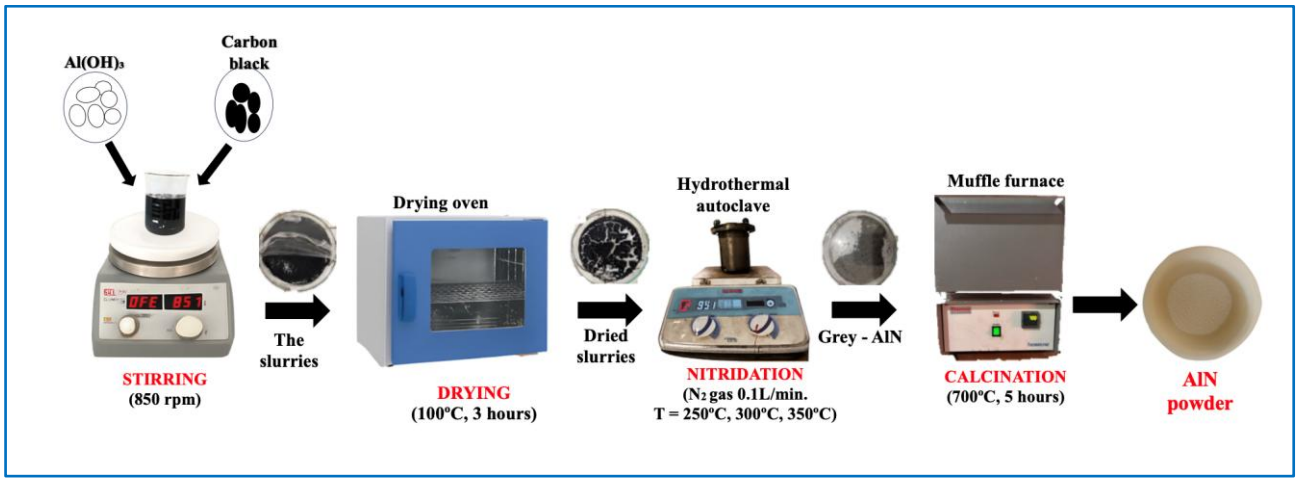

Figure 1 Sketch of AlN synthesis using a hydrothermal autoclave.

Characterization of Nano-Aluminium Nitride

Chemical and structural characterization

The characterization of chemical composition was conducted using Bruker Alpha II FTIR spectroscopy. The spectral range chosen for analysis was from 400 cm^{-1} to 1,000 cm^{-1}.

X-ray diffraction (XRD) (PANalytical, Almelo, Netherlands) served as the basis for crystallographic investigation on the synthesized AlN. To analyze the crystallite size of the microsphere on the formation of AlN, the Debye–Scherrer equation was used as described in Eq. (3) [28].

$$D = \frac{k.\lambda}{\beta.cos\theta} \quad (3)$$

where; D = Diameter of particle, k = Debye–Scherrer constant (0.89), λ = X-ray wavelength (1.54060 Å), β = FWHM, and θ = Bragg angle.

Morphology and particle size

SEM (Hitachi SU3500, Tokyo, Japan) was used to observe the morphology of aluminium nitride, and the particle size was observed using PSA (HORIBA SZ-100) with a measurement accuracy of 100 nm = ±2%.

Ultraviolet spectroscopy

UV-Vis spectroscopy (Edinburgh DS5) was used to assess the optical characteristics of aluminium nitride. The results of AlN absorbance were analyzed using the Tauc Plot's methods to determine the bandgap energy as described in Eq. (4) [29].

$$(\alpha h\nu)^2 = A(h\nu - Eg) \quad (4)$$

where: α = coefficient of absorbance (α = 2.303 A), h = Planck's constant, v = light frequency (hν = 1,240/λ), λ = wavelength (nm) and Eg = band gap energy (eV).

Results and discussion

Chemical and structural characterization

FTIR and XRD investigations were performed on synthesized samples to investigate the impact of molar ratio of $Al(OH)_3$:C and nitridation temperature on aluminium nitride (AlN) formation.

FTIR analysis

Characterization results of aluminium nitride synthesis, employing mass ratios of $Al(OH_3)$:C of 3:1, 4:1 and 5:1 with nitridation conducted at a temperature of 300 °C using a hydrothermal autoclave shown in **Figure 2(a)**. This characterization serves as an initial screening to ascertain the most optimal mass ratio for aluminium nitride synthesis via the CRN–hydrothermal autoclave-assisted method. The results indicate that aluminium nitride starts formation within the wavelength range of 200 - 300 cm^{-1}. The maximum absorption peak of Al-N bonds is observed at 488 cm^{-1} for mass ratio 3:1, 485 cm^{-1} for mass ratio 4:1 and 480 cm^{-1} for mass ratio 5:1. The peaks at ~ 2,152 cm^{-1}, ~ 1,979 cm^{-1} and ~ 1,626 cm^{-1} indicate the presence of OH bending vibrations resulting from the absorption of H_2O molecules or remaining O-H compounds in the precursor. This is in accordance with research findings from [30,31]. Due to sample with mass ratio 3:1

exhibiting the broadest peak, its mass ratio of $Al(OH)_3$:C (3:1) was selected as the precursor reference for nitridation analysis by hydrothermal autoclave at varying temperatures of 250 and 350 °C.

From **Figure 2(b)**, mass ratio 3:1 and nitridation temperature varies from 250 °C, 300 °C and 350 °C. The results show that in all spectra, the low wavenumber area (400 - 700 cm^{-1}) exhibits characteristics associated with Al–N stretching vibrations, notably near 490 cm^{-1}, thereby affirming the existence of AlN. The peak exhibits its lowest intensity at 250 °C (483 cm^{-1}), increases at 300 °C (488 cm^{-1}) and reaches maximum intensity at 350 °C, signifying the gradual production of Al–N bonds with rising nitridation temperature. This is in accordance with the research from [32]. Where the research indicates that elevated peaks are achieved at higher aluminium nitride synthesis temperatures, specifically 800 ºC, in contrast to synthesis at 400 ºC.

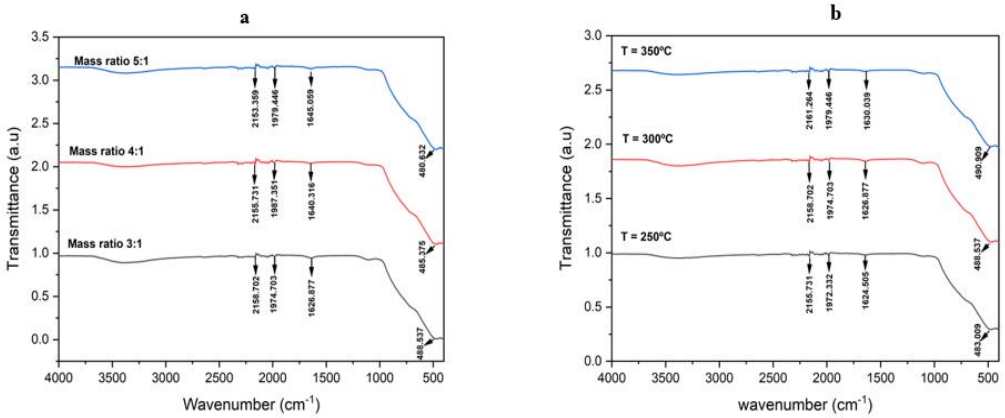

Figure 2 FTIR spectra of AlN powder. (a). Mass ratio of $Al(OH)_3$:C = 3:1, 4:1, 5:1, nitridation temperature at 300 °C. (b). Nitridation temperature at 250 °C, 300 °C and 350 °C, mass ratio of $Al(OH)_3$:C = 3:1.

XRD analysis

Figure 3 illustrates the XRD pattern of the nitridized product with different nitridation temperatures and a mass ratio of $Al(OH)_3$:C = 3:1. The XRD patterns exhibit a distinct evolution in phase composition and crystallinity as the nitridation temperature increases. The diffraction peaks are comparatively broad and weak at 250 °C, indicating the presence of predominantly amorphous or weakly crystalline phases. Several pointed reflections that correspond to γ-Al_2O_3 are still observed, indicating that the transformation of aluminium hydroxide to AlN is still incomplete at this particular stage. The characteristic diffraction peaks of AlN are not clearly visible and are barely detectable. With the temperature nitridation of 300 °C the strength of the AlN peak becomes more prominent, while the Al_2O_3 reflection decreases, signifying a partial conversion of the oxide phase into AlN. The diffraction peaks sharpen and shift slightly, signifying the formation of a more organized AlN crystalline structure.

At 350 °C, the XRD pattern indicates a significant enhancement in the purity and crystallinity of the AlN phase. The AlN peak is predominant, accompanied by significantly decreased background noise and negligible residual oxide phase peaks. This indicates that 350 °C is the best temperature within the examined range for the effective nitridation of $Al(OH)_3$ and carbon into crystalline AlN.

The phase evolution in XRD (**Figure 3**) aligns with the thermodynamic reaction pathway: $Al(OH)_3 \rightarrow Al_2O_3 \rightarrow AlON \rightarrow AlN$.

At a temperature of 250 °C its was predominantly composed of Al_2O_3, as it is expected that at low temperatures, the CRN reaction remains unfavorable. At a temperature of 300 °C, wurtzite AlN peaks (about 39.6°, 45.6°, 55.7°, 66.9°) are observed alongside Al_2O_3, signifying partial conversion through the intermediate phase AlON. At the temperature of nitridation 350 °C, AlN is the predominant phase, suggesting that precursor activation through hydrothermal methods (formation of porous γ-Al_2O_3 and uniform carbon coating) decreased

diffusion barriers and activation energy, facilitating AlN formation at 250 - 350 °C, significantly lower than the traditional CRN temperature exceeding 1,500 °C. This phenomenon implies that the hydrothermal autoclave-assisted CRN approach significantly reduces the kinetic barrier by generating reactive γ-Al_2O_3 precursors and improving Al_2O_3–C interaction, therefore allowing AlN synthesis at 250 - 350 °C, far lower than the over 1,500 °C generally necessary for CRN methods [12,22].

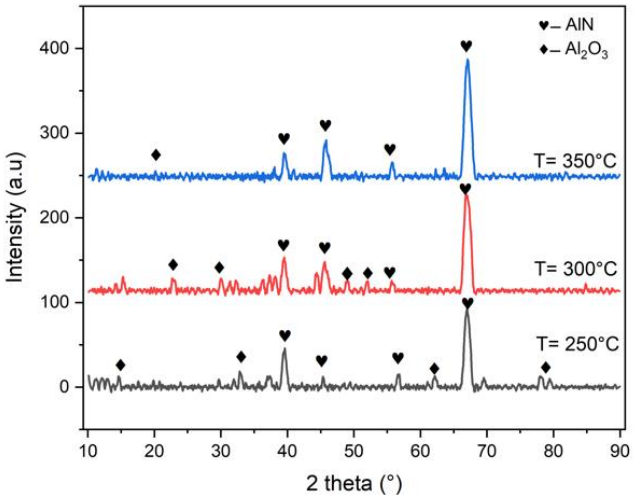

Figure 3 XRD result of AlN with nitridation temperatures at 250 °C, 300 °C and 350 °C (mass ratio of $Al(OH)_3$:C = 3:1).

The characteristics and hkl plane of aluminium nitride from temperature nitridation of 350 °C were detected at 39.48 º, 45.83 º, 55.78 º and 67.08 º (this was in agreement with JCPDS No. 25-1133) with the d-spacing values of 2.28 Å, 1.98 Å, 1.65 Å and 1.39 Å. From the Debye–Scherrer equation Eq. (3), the crystallite size of AlN was ascertained to be about 10.55 nm, with the total crystallization about 67.04%. **Table 2** showed the detail of the hkl plane.

Table 2 hkl plane of AlN peaks with mass ratio of $Al(OH)_3$:C = 3:1; temperature nitridation of 350ºC.

No.	2 Theta (°)	FWHM	hkl	d-spacing [Å]	Crystallite size (nm)
1	39.48	0.7013	101	2.28	12.04
2	45.83	0.9929	102	1.98	8.69
3	55.78	0.6732	102	1.65	13.35
4	67.08	1.1746	200	1.39	8.11
		Mean			10.55

Both the FTIR and XRD study results indicate that temperature nitridation significantly impacts the AlN synthesis process using the CRN method. Higher temperatures will enhance the purity of the synthesis process. This aligns with findings that a greater quantity of AlN fibers is produced at elevated nitridation temperatures (1,700 °C to 1,600 °C) [10]. The structural investigations verify that the hydrothermal autoclave-assisted CRN method enhances AlN synthesis at significantly lower temperatures. The XRD data for the mass ratio $Al(OH)_3$:C = 3:1 at 350 °C reveal crystalline AlN with an average crystallite size of approximately 10.55 nm and a crystallinity of about 67.04%. This is far smaller than the crystallite sizes reported in conventional CRN research, which often span from 100 to 200 nm, even at temperatures above 1,200 - 1,500 °C [17,33]. This study shows that similar or even enhanced nanostructure crystallite sizes may be attained at 250 - 350 °C, highlighting the significant impact of hydrothermal activation on precursor reactivity.

Morphology and particle size

SEM and PSA were employed to investigate the particle morphology and dimensions of aluminium nitride synthesized at nitridation temperatures of 250 °C, 300 °C and 350 °C, with mass ratio of 3:1.

SEM image

Figure 4 illustrates the morphological results of the SEM image. The results indicate that the three samples still include major particle clusters, signifying agglomeration. The distribution of particles less than 1 µm in sample AlN with nitridation temperature of 250 ºC appears uneven and slightly structured. As the nitridation temperature rises (300 ºC and 350 ºC,), the frequency of agglomeration decreases significantly. Among the three sample types, sample E exhibits the most favorable results, characterized by a more heterogeneous particle distribution with diameters < 1 µm.

The SEM image indicates that AlN synthesis by the hybrid CRN-hydrothermal autoclave method at low nitridation temperatures is achievable.

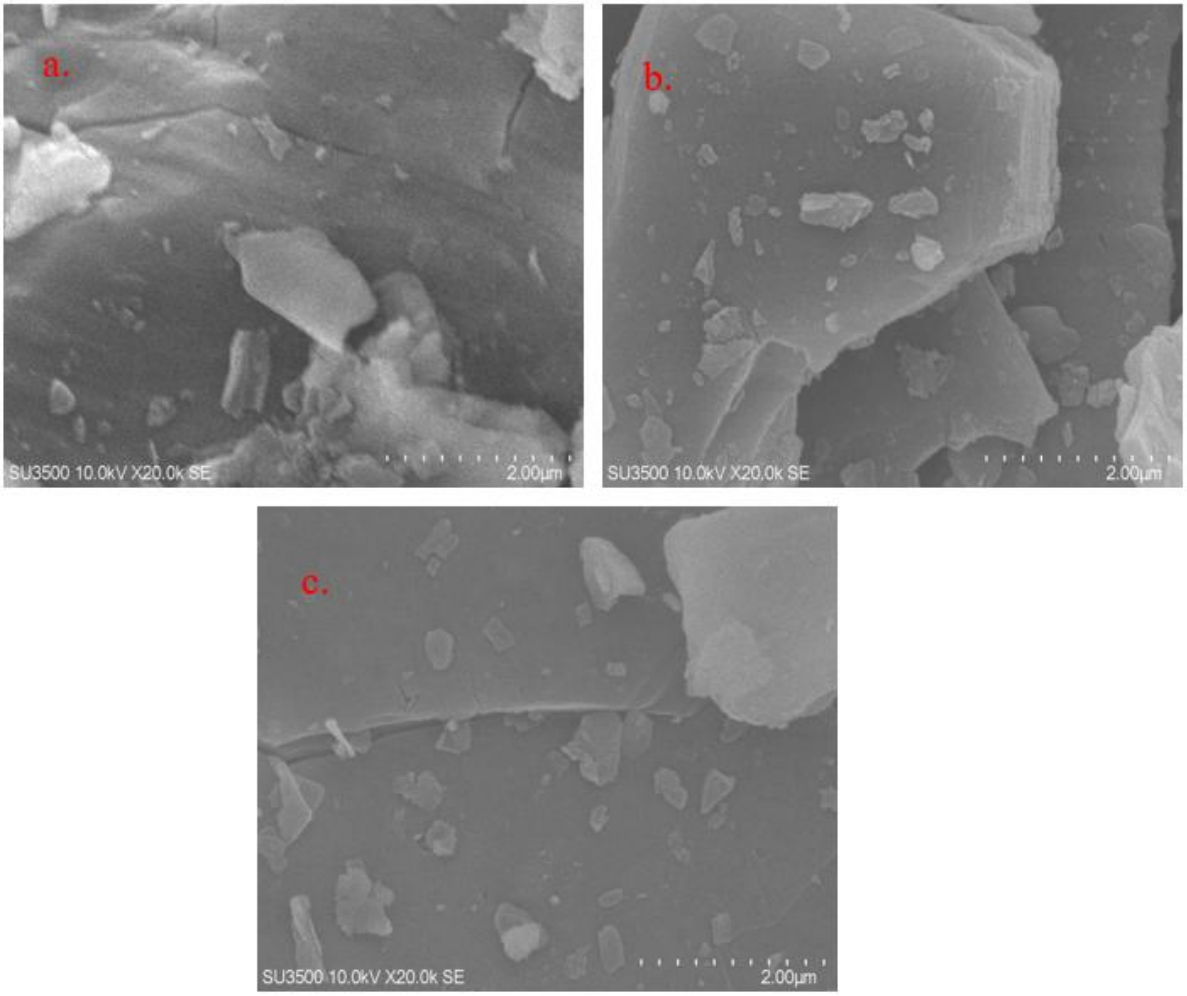

Figure 4 SEM photograph of the microstructure of AlN with mass ratio $Al(OH)_3$:C = 3:1. (a). Temperature nitridation 250 °C, (b). Temperature nitridation 300 °C, (c). Temperature nitridation 350 °C.

PSA analysis

Along with SEM image, particle size analysis (PSA) was performed on sample AlN at nitridation temperature 350 ºC and mass ratio $Al(OH)_3$:C = 3:1 **(Figure 5)**. The results indicate that the particle size achieved by the CRN-hydrothermal autoclave hybrid technique can attain an average of about 125.6 nm, PI = 2.838, with the highest diameter frequency about 171.25 nm. Although not merely under 100 nm, these findings indicate a substantial enhancement compared to

traditional CRN-derived powders. In contrast to literature reports of 150 - 200 nm particles [10,18], these results demonstrate less agglomeration attributable to hydrothermal preparation. This exhibits the efficacy of this method in synthesizing AlN at a submicron or nanostructure level at ultra-low temperature.

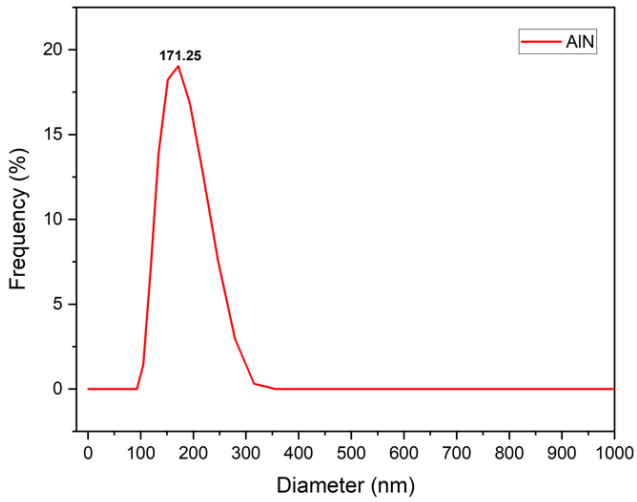

Figure 5 Particle size diameter with mass ratio of $Al(OH)_3$:C = 3:1; temperature of nitridation 350 °C.

Ultraviolet spectroscopy

Ultraviolet spectroscopy testing was conducted using UV-Vis spectrophotography to analyze the absorbance and energy of the optical band gap of aluminium nitride synthesized via the hybrid CRN-hydrothermal autoclave technique. **Figure 6** illustrates the UV-Vis testing results for synthesized AlN with mass ratios of $Al(OH)_3$:C = 3:1, 4:1 and 5:1. It demonstrated an absorption peak in the solar-blind area, which is about 300 nm. Furthermore, the energy bandgap of the material was calculated using the Tauc Plot's method in Eq. (4) and the result showed a bandgap energy of 5.56 eV (mass ratio 3:1) and for mass ratios 4:1 and 5:1, it was 5.55 eV and 5.31 eV.

The comparison of several bandgap energies from different AlN is shown in **Table 3**.

Table 3 Band Gap energies from several AlN.

Reference	Method	Sample / Preparation	Band Gap (eV)	Highlight
This work (2025)	UV–Vis spectroscopy	AlN synthesized using hydrothermal autoclave-assisted CRN (250 - 350 °C)	5.31 - 5.56 eV	Exhibited low-temperature synthesis of AlN with preserved optical characteristics and nanostructure.
Bakalova *et al.* [32]	VIS/IR spectroscopic ellipsometry	AlN grown using pulsed-laser-deposited (PLD)	4.2 eV; 6.2 eV	N_2 pressure and temperature influencing the Band Gap energy
Choudhary *et al.* [34]	Spectroscopic ellipsometry	AlN thin films using pulsed DC magnetron sputtering	5.0 - 5.48 eV	Band Gap decreased by increasing N_2/Ar flow ratio
Lee *et al.* [35]	UV–Vis spectroscopy	Nanovoid-assisted AlN crystal	6.08 eV	Regrown AlN suits for solar blind photodetector
Sohai *et al.* [36]	UV-vis spectroscopy	Gas-source molecular beam epitaxy	6.1 eV	Dependence of band gap on temperature
Silveira *et al.* [37]	Cathodoluminescence, transmission/absorption	Bulk AlN single crystal	6.0 - 6.03 eV	Dependence of band gap on temperature

The present research reports an optical band gap of AlN (5.31 - 5.56 eV). This bandgap energy is lower than the bandgap energy of AlN commercially reported, i.e., 6.2 eV. This result is similar to the reported bandgap with a lower nitridation temperature; the energy bandgap produced is also lower. (BG = 4.2 eV at T =

400 °C; BG = 6.2 eV at T = 800 °C) [32]. A band gap range of 5.0 - 5.48 eV for AlN thin films produced with pulsed DC magnetron sputtering was observed, indicating that the band gap diminished with an increasing N_2/Ar ratio due to alterations in stoichiometry and oxygen incorporation. [35]. This range of band gap results aligns with the present study, indicating that the hydrothermal autoclave–CRN approach can yield equivalent optical characteristics without requiring high vacuum or sputtering conditions. In contrast, higher band gap energies observed using bulk AlN revealed that the band gap depends on temperature [36-38].

The significantly reduced band gap identified in our investigation is ascribed to nanoscale phenomena and potential defect states intrinsic to low-temperature synthesis. The nanostructured AlN retains the wide-band-gap characteristics essential for deep-UV optoelectronic applications, in contrast to high-quality bulk crystals. These comparisons indicate that the band gap values obtained in this study align with those of AlN produced by higher-energy methods, while additionally confirming that low-temperature synthesis techniques may maintain the fundamental optical features of AlN. This ultra-wide bandgap of AlN (~6.2 eV) qualifies it as a formidable candidate for deep-UV device applications. High-quality AlN thin films with these bandgaps have been utilized in far-UV photodetectors, exhibiting sharp cutoff edges (~206 nm) and exceptional responsivity [38]. Simultaneously, deep UV LEDs based on core−shell nanostructures of AlN with UV emission of 229 nm have been developed [39]. The presented device outcomes underscore the promise of nanoscale AlN, synthesized using hydrothermal autoclave-assisted CRN, for UV optoelectronics.

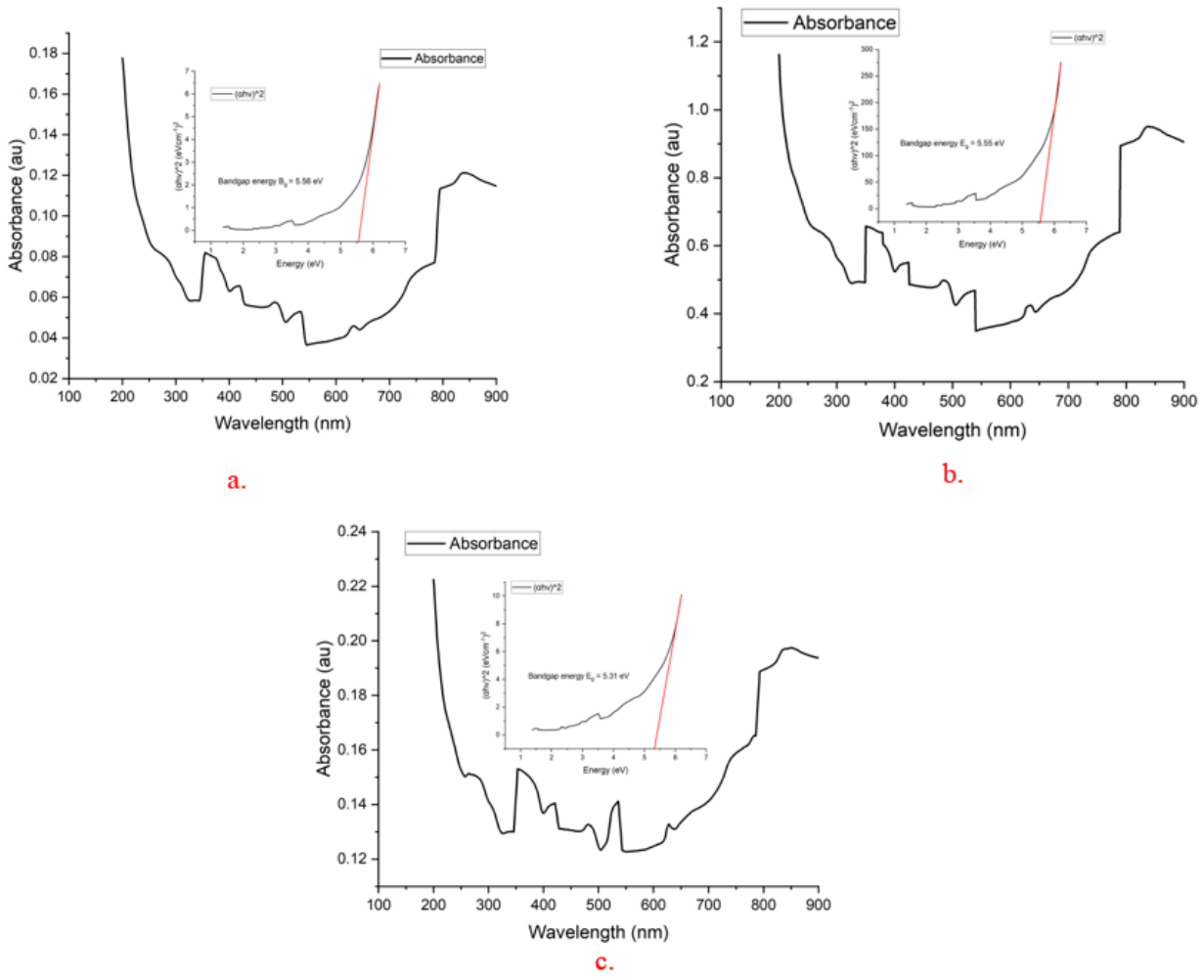

Figure 6 Absorbance and bandgap energy of synthesized AlN. (a) Mass ratio of $Al(OH)_3$:C = 3:1. (b) Mass ratio of $Al(OH)_3$:C = 4:1. (c) Mass ratio of $Al(OH)_3$:C = 5:1

Table 4 Comparison of several AlN synthesis with CRN methods.

References	Precursor	Method	Nitridation Temp (°C)	Particle Size	AlN Phase
Li *et al.* [1]	$NaAlO_2$+Carbon black	CRN+ball milling	800 – 1,600	0.5 - 0.18 µm	high-purity aluminum nitride (AlN) powder
He *et al.* [7]	$Al(NO_3)_3{\cdot}9H_2O$+$CO(NH_2)_2$+$C_6H_{12}O_6{\cdot}H_2O$	CRN+sol gel (Argon atmosphere)	1,000 - 1,300	20 - 30 nm	AlN spherical granule
Hao *et al.* [10]	Al_2O_3+Graphite felt	CRN+ball milling	1,600 - 1,900	~ 200 nm	AlN whisker, high purity and crystallinity
Li *et al.* [12]	Al_2O_3+Carbon black	CRN+ball milling+foaming	1,550 - 1,650	0.91 µm	High intrinsic AlN
Xu *et al.* [13]	Al_2O_3+Carbon black	CRN under vacuum condition	1,650	45 - 200 nm	Pure AlN, ultrafine
Xu *et al.* [14]	Al_2O_3+Carbon black	CRN+micro emulsion	1,550	~ 5 µm	Spherical AlN powder
Lee *et al.* [15]	α-Al2O3+Carbon black	CRN+additive (CaF_2, AlF_3, $Y(NO_3)_3$, $Ca(NO_3)_2$, and $Mg(NO_3)_2$)	1,500 – 1,650	0.38 -0.52 µm	Pure AlN powder
Wen *et al.* [17]	$Al(OH)_3$+Carbon black	CRN+ball milling+pvb additive	1,550	1.6–2 µm	Hexagonal AlN, homogenous particle
Sakthisabarimoorthi *et al.* [27]	$Al(NO_3)_3{\cdot}9H_2O$+CH_4N_2O+$C_{12}H_{22}O_{11}$	CRN+Hydrothermal	1,500	5 µm	Hollow AlN
This study	$Al(OH)_3$+Carbon black	CRN slurries+hydrothermal autoclave	350	~ 125 nm	Homogenous Pure AlN

The results of AlN synthesis using various CRN methodologies are compared in **Table 4**.

Most previous research utilized high nitridation temperatures, typically over 1,400 °C, to attain complete conversion or the synthesis of AlN with exceptional crystallinity and purity. $NaAlO_2$ and Al_2O_3 precursors are used for synthesizing AlN with ball milling addition, achieving high purities of AlN powder and whisker at temperatures about ~1,600 °C; however, the resultant particle sizes were comparatively large [1,10]. To reduce the particle size and enhance phase purity by employing additives such as CaF_2 and other promoters [15,17] or other methods such as the addition of microemulsion and foaming agent CRN [12,14]. These experiments produced nanostructure or sub-micron particles (< 1,000 nm) but frequently necessitated supplementary processes, such as specialized apparatus to make foaming reagent in surface modification of the precursor and many different materials for the microemulsion, thus complicating scalability. Additionally, AlN with a spherical granule morphology of 20 - 30 nm via the sol-gel route-CRN was successfully synthesized. The nitriding temperature is lower than that of conventional CRN; nevertheless, it requires additional components and the development of sol-gel processes in an argon atmosphere. This constitutes a deficiency in a substantial quantity of equipment inventory. [7]. In contrast, the present study effectively illustrates the synthesis of homogenous hexagonal AlN at notably reduced temperatures (250 - 350 °C) through the integration of the CRN approach with a hydrothermal autoclave process. This method effectively attains a particle size of approximately 125 nm, equivalent to the outcomes of more energy-intensive procedures. Furthermore, the AlN synthesized at 350 °C exhibited a uniform and phase-pure structure, demonstrating the efficacy of the technique in regulating

morphology and improving nitridation efficiency, even at reduced temperatures.

From the result and comparison with other studies, it is highlighted that although conventional or modified CRN methods require high nitridation temperatures (> 800 – 1,500 °C), this study using the hybrid hydrothermal autoclave-assisted CRN method allows the synthesis of nanostructure AlN at temperatures of only 250 - 350 °C. This innovative method exhibits one of the initial examples of AlN synthesis at significantly lower temperatures. The hydrothermal process produces a reactive γ-Al_2O_3 precursor characterized by better homogeneity and less agglomeration, resulting in nanoscale crystallite dimensions while maintaining optical characteristics. This significant reduction in synthesis temperature not only improves understanding of precursor activation and reaction mechanisms but also provides practical benefits for the efficient production of AlN powder for electrical, thermal management and deep-UV optoelectronic applications. As previously stated, in addition to its application in optoelectronics, nano AlN is extensively utilized as a PCM composite filler due to its high thermal conductivity and structural stability, making it a prevalent choice for PCM composites in thermal energy storage [2-4].

This study is preliminary research aimed at proving the effectiveness of hydrothermal autoclave-assisted CRN in synthesizing nanoscale AlN. The characterization process encounters limitations due to the available circumstances and equipment, including Transmission Electron Microscope (TEM), surface energy thermodynamics analysis, X-ray Photoelectron Spectroscopy (XPS) and Photoluminescence (PL). Further studies will try to solve these limitations.

Conclusions

In this study nanoscale Aluminium nitride (AlN) was effectively synthesized using a novel hybrid method that integrates hydrothermal autoclave-assisted processing with the carbothermal reduction nitridation (CRN) method. AlN was effectively formed at significantly lower nitridization temperatures (250 - 350 °C) than the conventional CRN route (> 1,400 °C).

From structural analysis using FTIR and XRD, it was discovered that the formation of pure AlN phase and Al–N bonds increased with increasing temperature. At 350 °C and a mass ratio of $Al(OH)_3$:C = 3:1, a homogeneous and crystalline AlN phase with minimal residual Al_2O_3 content was obtained. The crystallite size was about ~ 10.5 nm and the total crystallization percentage about 67.04%, yielding the most optimal results. In addition, from SEM and PSA results, nanostructured particles with an average size of about ~ 125 nm and further reduction in aggregation were observed.

Furthermore, the UV–Vis spectroscopy revealed an optical bandgap of approximately 5.6 eV, which, although lower than the theoretical value of AlN (~6.2 eV), is still consistent with the typical semiconductor behavior of AlN and still supports potential applications in electrical, thermal management and deep-UV optoelectronic applications. Compared to other methods that have been reported, this method provides a synthesis route that is more energy-efficient, scalable and environmentally friendly. It also involves fewer processing steps and reduced operational costs.

Acknowledgements

This study is part of a doctoral study in Program Studi Doktor Ilmu Teknik, Udayana University, Indonesia. Gratitude is expressed to FINDER U-CoE for the access and laboratory facilities. There is no funding or grant for this research.

Declaration of generative AI in scientific writing

The author declares that the use of AI tools (i.e., Grammarly and QuillBot) was used to improve the readability of the sentence and language in the manuscript with full human control. No AI tools are listed as author or co-author. All of the scientific content, interpretation and conclusions were developed by the authors.

CRediT author statement:

I Kadek Ervan Hadi Wiryanta: Conceptualization, Methodology, Investigation, Formal analysis, Writing - Original Draft. **Wayan Nata Septiadi**: Methodology, Supervision, Data Curation, Validation, Writing - Review & Editing. **Tjokorda Gde Tirta Nindhia**: Methodology, Supervision, Data Curation, Validation, Writing - Review & Editing. **I Made Joni**: Conceptualization, Methodology, Resources, Supervision, Data Curation, Validation, Writing - Review & Editing.

References

[1] G Li, B Li, B Ren, H Chen, B Zhu and J Chen. Synthesis of aluminum nitride using sodium aluminate as aluminum source. *Processes* 2023; **11(4)**, 1034.

[2] Q Huang, J Deng, X Li, G Zhang and F Xu. Experimental investigation on thermally induced aluminum nitride based flexible composite phase change material for battery thermal management. *Journal of Energy Storage* 2020; **32**, 101755.

[3] E Wondu, W Lee, M Kim, D Park and J Kim. Phase change materials for energy storage applications from PEG and PBAT with AlN and CNT as Fillers. *ACS Omega* 2024; **9(50)**, 49557-49565.

[4] A Tang, W Chen, X Shao, Y Jin, J Li and D Xia. Experimental investigation of aluminum nitride/carbon fiber-modified composite phase change materials for battery thermal management. *International Journal of Energy Research* 2022; **46(9)**, 12737-12757.

[5] X Wu, C Deng, J Di, J Ding, H Zhu and C Yu. Fabrication of novel AlN-SiC-C refractories by nitrogen gas-pressure sintering of Al_4SiC_4. *Journal of the European Ceramic Society* 2022; **42(8)**, 3634-3643.

[6] X Zeng, Y Wu, G He, W Zhu, S Ding and Z Zeng. High-pure AlN crystalline thin films deposited on GaN at low temperature by plasma-enhanced ALD. *Vacuum* 2023; **213**, 112114.

[7] Q He, M Qin, M Huang, H Wu, H Lu, H Wang, X Mu,Y Wang and X Qu. Synthesis of highly sinterable AlN nanopowders through sol-gel route by reduction-nitridation in ammonia. *Ceramic International* 2019; **45(12)**, 14568-14575.

[8] MI Lerner, EA Glazkova, AS Lozhkomoev, NV Svarovskaya, OV Bakina, AV Pervikov and SG Psakhie. Synthesis of Al nanoparticles and Al/AlN composite nanoparticles by electrical explosion of aluminum wires in argon and nitrogen. *Powder Technology* 2016; **295**, 307-314.

[9] S Rogers, M Dargusch and D Kent. Impacts of temperature and time on direct nitridation of aluminium powders for preparation of AlN reinforcement. *Materials* 2023; **16(4)**, 1583.

[10] X Hao, S Wan, W Kang, J Zhao, S Han, D Peng, P Yang and Q Wang. Carbothermal synthesis of high-aspect-ratio AlN whiskers using graphite felt as carbon source. *Ceramic International* 2022; **48(7)**, 9842-9847.

[11] KB Lee, J Kim, CH Shim, Y Kim, H Choi and JP Ahn. Low-temperature synthesis of high-purity AlN from Al powder. *Journal of Materials Research and Technology* 2022; **21**, 4526-4536.

[12] J Li, H Chen, G Zhou, D Huang, L Ling and X Qin. Synthesis of fine AlN powders by carbothermal reduction and nitridation from nano-alumina/carbon foam. *Ceramic International*. 2025; **51(7)**, 8291-8298.

[13] Y Xu, Z Zhou, X Chen, C Han, B Yang, B Xu and D Liu. Ultrafine AlN synthesis by alumina carbothermal reduction under vacuum: Mechanism and experimental study. *Powder Technology* 2021; **377**, 843-846.

[14] J Xu, H Wang and Z Zhao. Preparation of spherical AlN powders by combined microemulsion method and carbothermal method. *Ceramic International* 2019; **45(10)**, 12708-12715.

[15] SM Lee, MT Ayman, SM Jang, S Park and DH Yoon. Synthesis of pure fine AlN powder via CRN using nitridation promoter. *Materials Today Communications* 2024; **41**, 110935.

[16] C Ma, Y Li, X Wu and Y Gao. Synthesis mechanism of AlN–SiC solid solution reinforced Al_2O_3 composite by two-step nitriding of Al–Si_3N_4–Al_2O_3 compact at 1,500 °C. *Ceramic International* 2022; **49(9)**, 22022-22029.

[17] Q Wen, P Wang, J Zheng, Y Ying, J Yu, W Li, S Che and L Qiao. Carbothermal reduction synthesis of aluminum nitride from $Al(OH)_3$/C/PVB slurries prepared by three-roll mixing. *Materials* 2021; **14(6)**, 1386.

[18] A Chu, L Zhang, R Ud-din and Y Zhao. Reaction model and mechanism of preparing (Al_2O_3 + C) precursor for carbothermal synthesis of AlN by a modified low temperature combustion synthesis method. *Materials* 2022; **15(18)**, 6216.

[19] Y Shan, G Hou, X Sun, X Han, C Hong, J Xu and J Li. One-step carbothermal reduction and nitridation (CRN) for fast fabrication of fine and single phase AlON powder by using hydrothermal synthesized α-Al_2O_3/C mixture. *Ceramic International* 2021; **47(13)**, 18012-18019.

[20] TQ Tazim, M Kawsar, MS Hossain, NM Bahadur and S Ahmed. Hydrothermal synthesis of nano-metal oxides for structural modification: A review. *Next Nanotechnology* 2025; **7**, 100167.

[21] EV Rusu, V Morari, T Guțul, V Ursaki and P Vlazan. Hydrothermal preparation of oxide (Ga_2O_3, ZnO, TiO_2) and derivative nanoparticles. *The Moldavian Journal of the Physical Sciences*. 2022; **21(1)**, 61-70.

[22] G Feng, J Yang, D Zhou, Q Chen, W Xu and Y Zhou. Mechanism for hydrothermal-carbothermal synthesis of AlN nanopowders. *Journal of Inorganic Materials* 2025; **40**, 104-110.

[23] T Yamakawa, J Tatami, K Komeya and T Meguro. Synthesis of AlN powder from $Al(OH)_3$ by reduction-nitridation in a mixture of NH_3-C_3H_8 gas. *Journal of the European Ceramic Society* 2006; **26(12)**, 2413-2418.

[24] A Hermawan, HW Son, Y Asakura, T Mori and S Yin. Synthesis of morphology controllable aluminum nitride by direct nitridation of γ-AlOOH in the presence of N_2H_4 and their sintering behavior. *Journal of Asian Ceramic Societies* 2018; **6(1)**, 63-69.

[25] AF Alkaim, TA Kandiel, FH Hussein, R Dillert and DW Bahnemann. Solvent-free hydrothermal synthesis of anatase TiO_2 nanoparticles with enhanced photocatalytic hydrogen production activity. *Applied Catalysis A: General* 2013; **466**, 32-37.

[26] RS Al-Shemary, AM Aljeboree and AF Alkaim. Microwave-assisted hydrothermal synthesis as a nanocomposite with superior adsorption capacity for efficient removal of toxic Maxillon blue (GRL) dye from aqueous solutions. *Eurasian Chemical Communications* 2023; **5(9)**, 832-841.

[27] A Sakthisabarimoorthi, MT Ayman, SS Ryu and DH Yoon. Synthesis of hollow AlN microsphere by hydrothermal and carbothermal reduction–nitridation hybrid technique. *Ceramic International* 2024; **50(19A)**, 35154-35160.

[28] R Febrida, A Cahyanto, E Herda, V Muthukanan, F Faizal, C Panatarani and IM Joni. Synthesis and characterization of porous $CaCO_3$ vaterite particles by simple solution method. *Materials* 2021; **14(16)**, 4425.

[29] H Zhong, F Pan, S Yue, C Qin, V Hadjiev, F Tian, X Liu, F Lin, Z Wang and J Bao. Idealizing Tauc Plot for accurate bandgap determination of semiconductor with UV-Vis: A Case study for cubic boron arsenide. *The Journal of Physical Chemistry Letters* 2023; **14(26)**, 6702-6708.

[30] R Dallaev, N Papěž, D Sobola, S Ramazanov and P Sedlák. Investigation of structure of AlN thin films using Fourier-transform infrared spectroscopy. *Procedia Structural Integrity* 2019; **23**, 601-606.

[31] C Balasubramanian, S Bellucci, G Cinque, A Marcelli, M Cestelli Guidi, M Piccinini, A Popov, A Soldatov and P Onorato. Characterization of aluminium nitride nanostructures by XANES and FTIR spectroscopies with synchrotron radiation. *Journal of Physics Condensed Matter* 2006; **18**, S2095-S2104.

[32] S Bakalova, A Szekeres, M Anastasescu, M Gartner, L Duta, G Socol, C Ristoscu and IN Mihailescu. VIS/IR spectroscopy of thin AIN films grown by pulsed laser deposition at 400 °C and 800 °C and various N_2 pressures. *Journal of Physics: Conference Series* 2014; **514**, 012001.

[33] Z Yang, X Hou and L Dai. Low-temperature synthesis of Nano-AlN based on solid nitrogen source by plasma-assisted ball milling. *Journal of Renewable Materials* 2023; **11(6)**, 2941-2951.

[34] RK Choudhary, P Mishra, A Biswas and AC Bidaye. Structural and optical properties of aluminum nitride thin films deposited by pulsed dc magnetron sputtering. *ISRN Materials Science* 2013; **2013**, 759462.

[35] M Lee, H Son, HY Lee, J Moon, H Kim, JI Park, Z Liu, MG Hahm, M Yang and UJ Kim. Nanovoid-driven highly crystalline aluminum nitride and its application in solar-blind UV photodetectors. *Journal of Materials Chemistry C* 2020; **8(41)**, 14431-14438.

[36] S Sohal, W Feng, M Pandikunta, VV Kuryatkov, SA Nikishin and M Holtz. Influence of phonons on the temperature dependence of the band gap of AlN and AlxGa1-xN alloys with high AlN mole fraction. *Journal of Applied Physic* 2013; **113(4)**, 043501.

[37] E Silveira, JA Freitas, SB Schujman and LJ Schowalter. AlN bandgap temperature

dependence from its optical properties. *Journal of Crystal Growth* 2008; **310(17)**, 4007-4010.

[38] T Li, Y Lu and Z Chen. Heteroepitaxy growth and characterization of high-quality AlN films for far-ultraviolet photodetection. *Nanomaterials* 2022; **12(23)**, 4169.

[39] PM Coulon, G Kusch, RW Martin and PA Shields. Deep UV emission from highly ordered AlGaN/AlN Core-Shell nanorods. *ACS Applied Materials and Interfaces* 2018; **10**, 33441-33449.